



Cairo University  
Journal of Advanced Research



## ORIGINAL ARTICLE

# Effect of P<sub>2</sub>O<sub>5</sub> and MnO<sub>2</sub> on crystallization of magnetic glass ceramics



Salwa A.M. Abdel-Hameed <sup>a,\*</sup>, Mohamed A. Marzouk <sup>a</sup>, Mohamed M. Farag <sup>b</sup>

<sup>a</sup> Glass Department, National Research Center, Dokki, Cairo, Egypt

<sup>b</sup> Biomaterial Department, National Research Center, Dokki, Cairo, Egypt

## ARTICLE INFO

*Article history:*

Received 8 May 2013

Received in revised form 4 July 2013

Available online 17 July 2013

*Keywords:*

X-ray method

Magnetic properties

Glass ceramics

Magnetite

## ABSTRACT

This work pointed out the effect of adding P<sub>2</sub>O<sub>5</sub> and/or MnO<sub>2</sub> on the crystallization behavior of magnetic glass ceramic in the system Fe<sub>2</sub>O<sub>3</sub>-ZnO-CaO-SiO<sub>2</sub>-B<sub>2</sub>O<sub>3</sub>. The differential thermal analysis of the quenched samples revealed decrease in the thermal effects by adding P<sub>2</sub>O<sub>5</sub> and/or MnO<sub>2</sub> to the base sample. The X-ray diffraction patterns show the development of nanometric magnetite crystals in a glassy matrix. Heat treatment at 800 °C for 2 h, under reducing atmosphere, caused an increase in the amount of the crystallized magnetite with the appearance of minor hematite and Ca<sub>2</sub>SiO<sub>4</sub>. The transmission electron microscope revealed a crystallite size in the range 10–30 nm. Magnetic hysteresis cycles were analyzed with a maximum applied field of 25 kOe at room temperature. The prepared magnetic glass ceramics are expected to be useful for localized treatment of cancer.

© 2013 Production and hosting by Elsevier B.V. on behalf of Cairo University.

## Introduction

Hyperthermia destroys cancer cells by raising the tumor temperature to a “high fever” range, similar to the way that the body naturally uses to combat other forms of disease [1]. Generally, tumors are more easily heated than the surrounding normal tissues, since blood vessels and nervous systems are poorly developed in the tumor, and cancer cells are easily killed by heat treatment, since oxygen supply via the blood vessels is not sufficient in the tumor. Hence hyperthermia is expected to be a most useful treatment for cancer with no side

effects [2]. On the contrary, these temperatures are safe for surrounding healthy tissues with normal and efficient blood cooling systems [2].

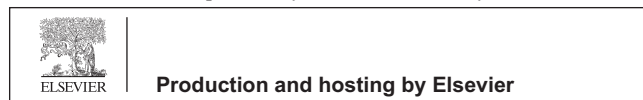
Bioactive ferromagnetic glass–ceramics are expected to be useful as thermoseeds for hyperthermia treatment of cancer, especially deep-seated cancers such as bone tumors. When ferromagnetic glass–ceramics are implanted around tumors in granular form, they are bonded to each other so as not to be moved by forming biologically active bone-like apatite on them [3], and stably fixed around the tumors if they are located near bones. Moreover, when they are placed under an alternating magnetic field, they generally heat effectively cancer cells to be necrotized by magnetic hysteresis loss. After heating, they can also reinforced weakened tumorous bone by bonding to bone.

Several materials that generate heat by hysteresis loss have been developed [4–9]. Among them, bioactive ferro and ferrimagnetic glass–ceramics have been investigated [10–13].

\* Corresponding author. Tel.: +20 33371312; fax: +20 33387803.

E-mail address: [Salwa\\_NRC@hotmail.com](mailto:Salwa_NRC@hotmail.com) (S.A.M. Abdel-Hameed).

Peer review under responsibility of Cairo University.



Preparation of magnetite-containing glass ceramics has been reported by several workers [2,14,15]. It is known that heat generation depends mainly on the magnetic properties of the implant, the magnetic field parameters and the characteristics of the tissue [16].

Bretcanu et al. [16] prepared ferrimagnetic bioglass-ceramics containing 45 wt% of magnetite revealing a saturation magnetization of 34 emu/g and a coercive force of 85 Oe. The estimated heat generation of this glass-ceramic using a magnetic field of 40 kA/m and a frequency of 440 kHz was 25 W/g. The previous material showed a bioactive behavior after 2 weeks of soaking in a simulated body fluid. Ebisawa et al., in 1997 [2] prepared glass ceramic contains 36% magnetite, in a matrix of CaO-SiO<sub>2</sub> based glass, and  $\beta$ -wollastonite which showed ferrimagnetisms and no bioactivity [17].

Kuwashita et al. [18] prepare zinc-iron ferrite (Zn<sub>x</sub>Fe<sub>3-x</sub>O<sub>4</sub>) in a CaO-SiO<sub>2</sub> glassy matrix by heat-treatment under 95 CO<sub>2</sub> + 5H<sub>2</sub> atmosphere. The prepared material showed a large amount of heat generation of 12.4 W g<sup>-1</sup> under conditions of 300 Oe and 100 kHz.

Wu et al. [19] found that, Zn ions play an important role in the human body, as reported to be involved in bone metabolism and can stimulate bone formation and increase bone protein, calcium content, and alkaline phosphates activity in humans and animals. They crystallize hardystonite (Ca<sub>2</sub>Zn-Si<sub>2</sub>O<sub>7</sub>) which might be biocompatible and used as biomaterials [19].

From all the above mentioned materials manganese zinc ferrite (Mn-ZnFe<sub>2</sub>O<sub>4</sub>) have special importance due to its high initial permeability, saturation magnetization and relatively lower eddy current loss compared to alloy cores [20], moreover Mn-Zn ferrites are very important in biomedicine as magnetic carriers, such as in bioseparation, enzyme and protein immobilization [21].

This work aimed at preparation and characterization of magnetic glass ceramic in the Fe<sub>2</sub>O<sub>3</sub>·ZnO·CaO·SiO<sub>2</sub>·B<sub>2</sub>O<sub>3</sub> system containing P<sub>2</sub>O<sub>5</sub> and MnO<sub>2</sub>. The influence of adding different addition from P<sub>2</sub>O<sub>5</sub> and/or MnO<sub>2</sub> on sequence of crystallization, amount and crystal size of the developed ferrite and microstructure were studied.

P<sub>2</sub>O<sub>5</sub> was added to study its effect as nucleating agents on the crystallization of magnetite, while MnO<sub>2</sub> were added to study the effect of replacing Fe<sup>2+</sup> by Mn<sup>2+</sup>, in the magnetite crystals, on the crystallization process.

## Experimental

### *Theoretical considerations on designing glass ceramic composition*

In previous work [22], the authors succeed to precipitate ~60% nanoparticles magnetite in two different systems, Fe<sub>2</sub>O<sub>3</sub>·CaO·ZnO·SiO<sub>2</sub>·B<sub>2</sub>O<sub>3</sub> and Fe<sub>2</sub>O<sub>3</sub>·CaO·SiO<sub>2</sub>·B<sub>2</sub>O<sub>3</sub>. The results showed that, crystallization of large amount of nanoparticles of magnetite in the presence of Zn ions; consequently the saturation magnetization was increased to reach 52.13 emu/g. In order to improve the amount and nano-crystallite size of magnetite, we got before in the Zn-containing sample, different oxides such as TiO<sub>2</sub>, Na<sub>2</sub>O and P<sub>2</sub>O<sub>5</sub> were added to this composition. The results showed that, addition

of the P<sub>2</sub>O<sub>5</sub> was greatly enhancing the amount and nano-crystallite size of magnetite.

### *Preparation of glasses*

The chemical compositions of the examined glasses are shown in Table 1. About 100 g powder mixtures of our compositions were prepared from reagent grades of CaO as Ca<sub>2</sub>CO<sub>3</sub>, SiO<sub>2</sub>, Fe<sub>2</sub>O<sub>3</sub>, ZnO and B<sub>2</sub>O<sub>3</sub> as H<sub>3</sub>BO<sub>3</sub>. Different amounts of MnO<sub>2</sub> (0.5–40 gm) as MnCO<sub>3</sub> and/or P<sub>2</sub>O<sub>5</sub> (3–10 gm) as NH<sub>4</sub>H<sub>2</sub>PO<sub>4</sub> were added over 100% batch composition.

Our target was to obtain a glass-ceramic, not a ceramic material, so a melting step was necessary. Based on their compositions, the batches were melted in a platinum crucible at 1350–1400 °C for 2 h in an electric furnace, with occasional swirling every 30 min to ensure homogenization. As the amount of P<sub>2</sub>O<sub>5</sub> and/or MnO<sub>2</sub> increased the melting temperatures decreased. The glass melted at 1400 °C was poured onto a stainless steel plate at room temperature and pressed into a plate 1–2 mm thick by another cold steel plate. An additional sample was poured at 1450 °C to study the effect of increasing temperature on the crystallization of magnetite.

### *Crystallization of glasses*

The samples were thermally examined using Differential Thermal Analysis (DTA). According to the DTA results the obtained samples were covered with active carbon powders, to apply a reducing atmosphere preventing ferrous ions from oxidation, and heated up to various temperatures at a rate of 10 °C min in a SiC electric furnace for crystallization. It was noticed that the synthesis parameters (such as temperature, time, heating rate, and atmosphere) play a fundamental role for magnetite crystallization.

### *Characterization*

The quenched samples were subjected to powder X-ray diffraction using Ni-filled Cu K $\alpha$  radiation for determining the types and contents of the precipitated crystalline phases. The average crystallite size of magnetite in the heat treated and untreated samples for the most intense peaks (220, 311, 400, 511 and 440) was determined from the XRD using Debye-Scherrer formula:  $D = k\lambda/B \cos \theta$ , where  $D$  is particle size,  $k$  is constant,  $\lambda$  for Cu is 1.54 Å,  $B$  is full half wide and  $2\theta = 4^\circ$ . The microstructures of prepared samples were studied using TEM. The sample was crushed and sonically suspended in ethanol and few drops of the suspended solution were placed on an amorphous carbon film held by copper microgrid mesh and then observed under transmission electron microscope.

## Results and discussion

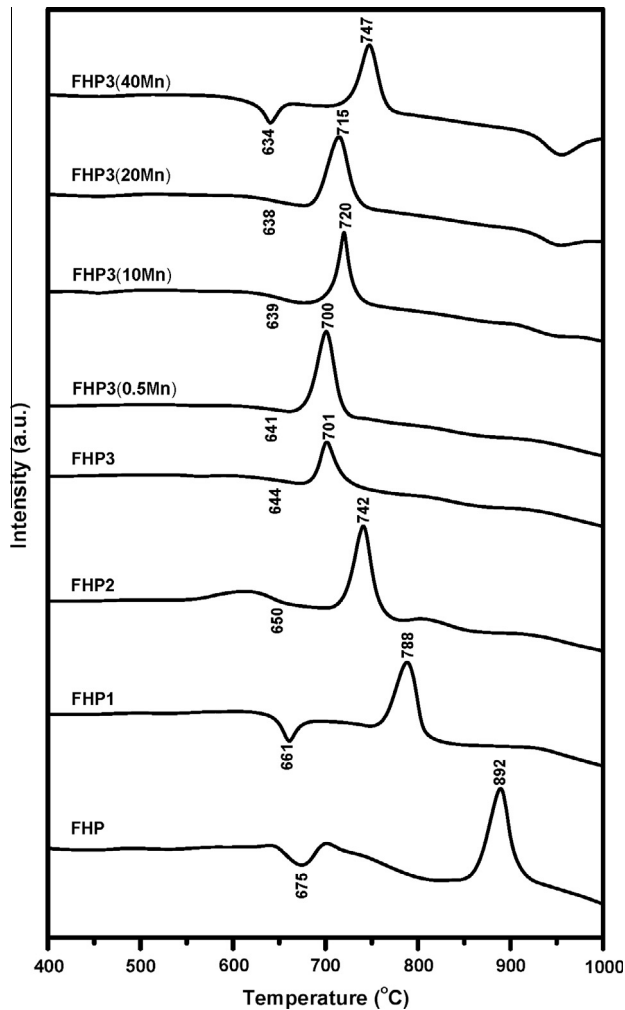
### *Characterization*

Fig. 1 shows thermal behavior of samples under investigation. All curves show a glass transformation temperature (T<sub>g</sub>) typical of an amorphous phase in the range of 634–675 °C and exothermic peak in the range of 700–892 °C. The transformation temperature is accompanied by absorption of the heat

**Table 1** Chemical composition of the studied glasses in wt%.

Sample	Fe <sub>2</sub> O <sub>3</sub>	CaO	ZnO	SiO <sub>2</sub>	B <sub>2</sub> O <sub>3</sub>	P <sub>2</sub> O <sub>5</sub> *	MnO <sub>2</sub> *
FHP	58.26	13.88	10.07	14.88	2.91	3	–
FHP1	58.26	13.88	10.07	14.88	2.91	5	–
FHP2	58.26	13.88	10.07	14.88	2.91	7	–
FHP3	58.26	13.88	10.07	14.88	2.91	10	–
FHPMn0.5	58.26	13.88	10.07	14.88	2.91	10	0.5
FHPMn10	58.26	13.88	10.07	14.88	2.91	10	10
FHPMn20	58.26	13.88	10.07	14.88	2.91	10	20
FHPMn 40	58.26	13.88	10.07	14.88	2.91	10	40

\* P<sub>2</sub>O<sub>5</sub> and MnO<sub>2</sub> were added above 100%.



**Fig. 1** Differential thermal analysis of samples under investigation.

required for rearrangement of different atoms as a pre-crystallization step. The presence of the glass transition temperature confirms the presence of reasonable amounts of residual amorphous phases for the glass-ceramic samples [23]. The glass transition temperatures of quenched samples are similar for glasses containing iron ions [24] especially for FHPMn40 sample (639 °C). T<sub>g</sub> was followed by an exothermic peak(s) corresponding to the crystallization process with an energy release. In general, a significant decrease in the thermal effects was observed by adding P<sub>2</sub>O<sub>5</sub> and/or MnO<sub>2</sub>.

The transformation temperature is known to be a good indicator for the relative amount of amorphous phase present in the samples. In the present study, an increase of both exothermic and endothermic peaks was noticed on samples contain MnO<sub>2</sub>, than base composition (FHP), thus indicate the mineralizing role of MnO<sub>2</sub> in enhancing the magnetite crystallization at the melting temperature. Consequently, the amount of the amorphous phase was decreased; leading to thermal transformation processes occur at higher temperatures. The increase in the area under the exothermic peak and consequently the enthalpy in FHPMn40 sample certify the above result.

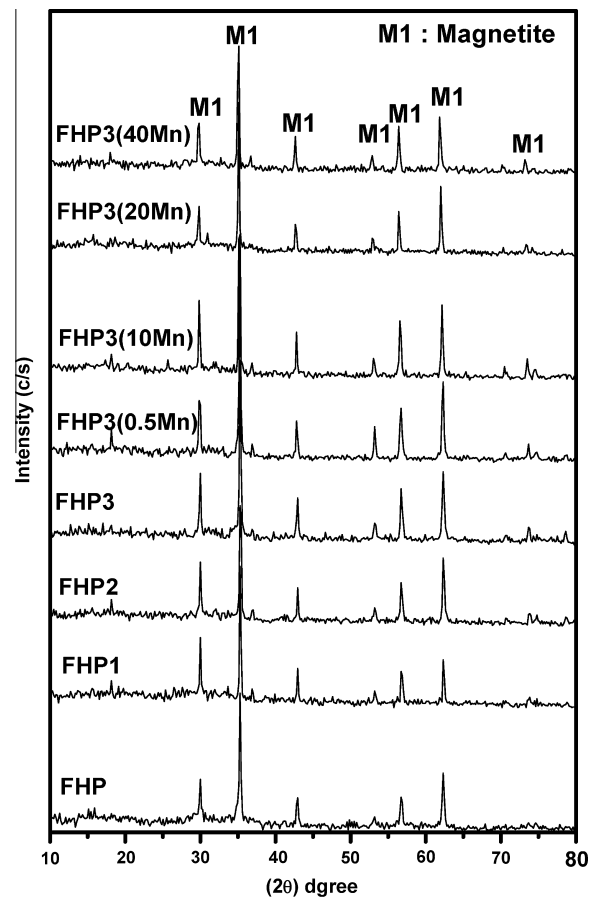


**Fig. 2** XRD of different samples after cooling from melting temperature.

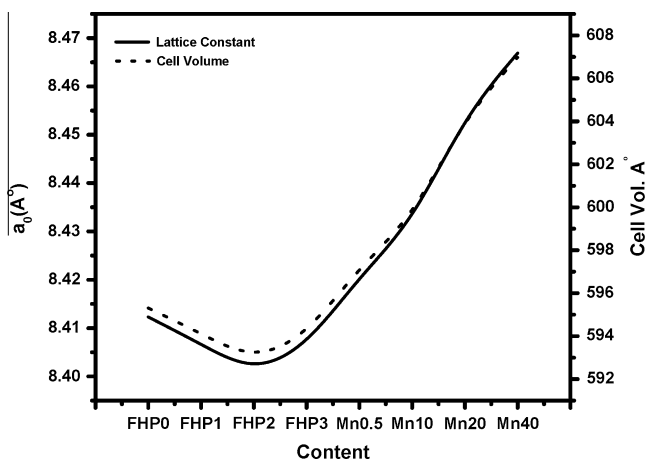


**Fig. 3** Effect of  $P_2O_5$  and  $MnO_2$  amount on the lattice parameters of crystallized ferrites after cooling from melting temperature.

From XRD results, the only crystallized phase after cooling from the melting temperature was magnetite. It can be clearly seen that, sharp peaks of all treated samples reflect high degree of crystallinity. Economically, although the samples melted at  $1450^\circ C$  showed slight higher magnetite peak intensities, only samples melted at  $1400^\circ C$  will be considered.

The X-ray diffraction patterns of glass-ceramics after cooling from melting temperature ( $1400^\circ C$ ) are shown in Fig. 2. The results present patterns corresponding to the common structure of magnetite ( $Fe_3O_4$ ) in a pure phase without any other phase's interference.

These XRD diagrams coincide with those reported in the previous work for the parent sample ( $Fe_3O_4$ ) [25]. They are dominated by a strong Bragg peak located at ca.  $2\theta = 35^\circ$  and peaks with medium intensity at  $30^\circ$ ,  $57^\circ$  and  $63^\circ$ . Considering the intensity and position of the peaks, it is well known that patterns of the Cubic unit-cell ( $Fd\bar{3}m$  space group) can be identified as magnetite phase.

Generally, the cumulative results of all samples were verified by cell volume calculation which revealed that, the cell volume increased by adding  $MnO_2$  and slightly decreased by adding  $P_2O_5$ . The explanation of the cell volume enlargement

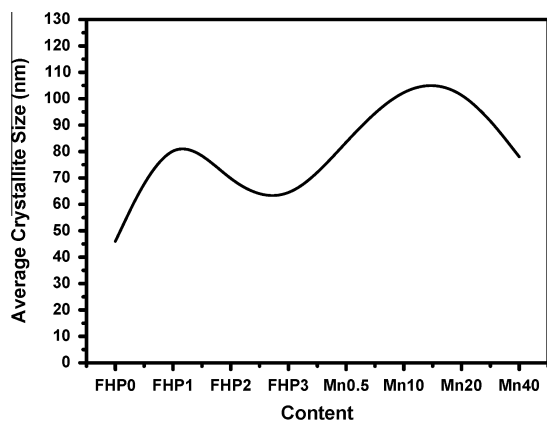


**Fig. 4** Effect of  $P_2O_5$  and  $MnO_2$  on the average crystallite size of crystallized ferrites after cooling from melting temperature.

could be explained as follows: the diffraction lines of the crystallized magnetite with an increasing amount of  $MnO_2$  were shifted to a higher d-spacing with an increase in the ( $a$ ) lattice parameter than that recorded in the reference data card of JCPDS (Joint Committee on Powder Diffraction Standards) which show a value of  $a_0 = 8.393\text{--}8.399 \text{ \AA}$ . This shift may be attributed to the incorporation of  $Mn^{2+}$  with its high ionic radii in the developed crystals of the magnetite solid solution (ss). Contrary, the  $P_2O_5$  addition caused slight lowering in the lattice parameter values of magnetite.

In order to illustrate how the unit cell and cell volume changes as a function of  $P_2O_5$  and  $MnO_2$  content, the lattice parameters  $a$ , and cell volume were determined as a function of  $P_2O_5$  and  $MnO_2$  content by the least-squares method, Fig. 3. The cubic parameters calculated via a least-squares refinement method using 14 well-defined XRD lines are  $a = 8.406$  (2) and  $a = 8.466$  (9)  $\text{\AA}$  for FHP3 and FHPMn 40, respectively. For these materials the spinal structure is well preserved upon considerable  $P_2O_5$  and  $MnO_2$  addition. As shown in Fig. 3, adding  $P_2O_5$  results in a slightly decrease of the cubic parameter; the  $a$ -axis shrinks can be explained as follow:  $P_2O_5$  provides an example of a network-former which exhibits the characteristics of nucleating agent. The phosphorus ion,  $P^{5+}$ , assumes tetrahedral co-ordination and therefore provides an example of phase separation due to a charge difference between the principal network-former,  $Si^{4+}$ , and the

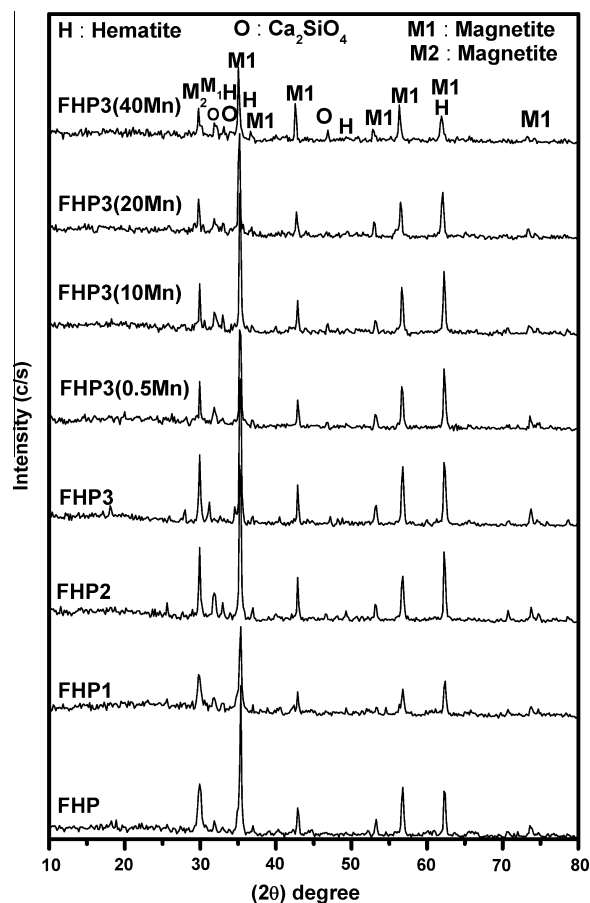


**Fig. 5** XRD patterns of different samples after heat treatment at  $800^\circ C$  for 2 h.

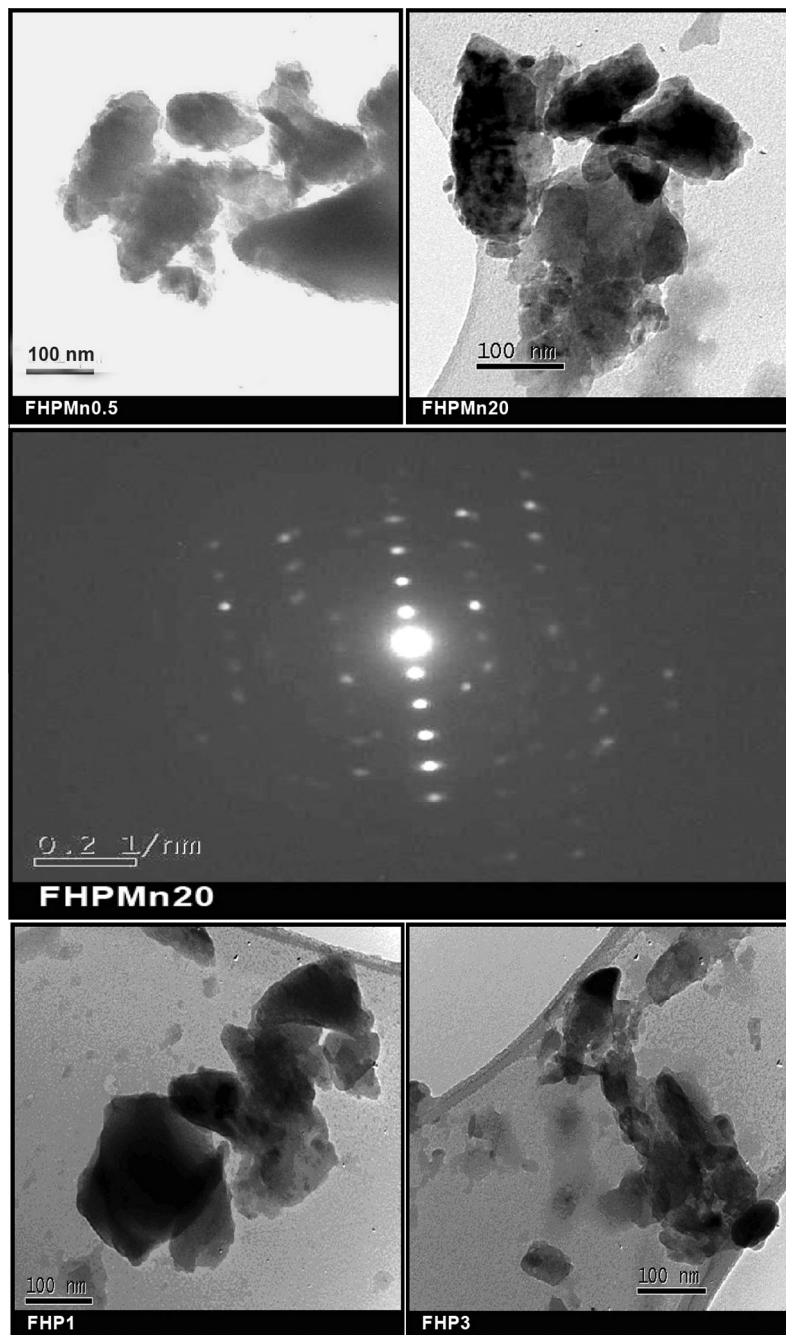


Fig. 6 TEM of different samples after cooling from melting temperature.

“foreign” network-former ions, P<sup>5+</sup> [26]. It is interesting to remark that the lattice parameter variations are very similar for the different dopant concentrations. On the contrary, adding Mn<sup>2+</sup> cations caused progressive increase in lattice parameter, where Mn<sup>2+</sup> which have large ionic radius (93 pm) replaced the lower ionic radius Fe<sup>2+</sup> ions (65 pm).

Several factors can contribute to the broadening of peaks in X-ray diffraction [25,27]. For example, the instrumental factors related to the resolution and the incident X-ray wavelength, as well as the sample factors such as crystallite size and non-uniform microstrain. In the case of an instrumental broadening, the line width will vary smoothly with  $2\theta$  or  $d$

spacing. On the other hand, the line broadening originating from the sample characteristics will have a different relationship. Combining the Scherrer's equation for crystallite size and the Bragg's law for diffraction, crystallite size and microstrain components are estimated by using the following equation:

$$B^2 \cos^2 \theta = 16 \langle e^2 \rangle \sin^2 \theta + \frac{K^2 \lambda^2}{L^2}, \quad (1)$$

where  $B$  is the full-width at half-maximum (FWHM) after correction of the instrumental broadening for finely powdered silicon powder,  $\theta$  is the diffraction angle,  $\langle e^2 \rangle$  denotes local

strains (defined as  $\Delta d/d$  being the interplanar spacing),  $L$  is the crystallite size and  $K$  is a near-unity constant related to crystallite shape.

Crystallite size obtained from XRD, Fig. 4 shows a common crystallization of magnetite nano particles ( $< 100$  nm). Increasing amount of  $\text{MnO}_2$  added leads to significant increase in the crystallite size which may attributed to the replacement of Fe ions (smaller ionic radius) by Mn ions (larger ionic radius).

The broadness of magnetite peaks shown in XRD data are in the order of  $\text{FHPMn}_{40} > \text{FHPMn}_{20} > \text{FHPMn}_{10} > \text{FHPMn}_{0.5}$  and consequently the crystallite size are increased in the same order.

Heat treatment of different samples at  $800^\circ\text{C}$  for 2 h under reducing atmosphere, Fig. 5 revealed increase in the magnetite phase and crystallization of minor hematite and calcium silicate ( $\text{Ca}_2\text{SiO}_4$ ). Two different structures of magnetite were developed. As the amount of magnetite increased there are chance to crystallize to different structure forms from magnetite.

Comparing the XRD patterns of glass-ceramics obtained by cooling of molten glass Fig. 1 and after the additional thermal treatment, Fig. 5, it can be concluded that, the difference in the relative amount of crystallized magnetite in the samples (in spite of containing the same amount of iron oxide) could be attributed to the effects of adding  $\text{MnO}_2$  on lowering the viscosity of the melt and formation of solid solution with magnetite, consequently, some iron oxides remain entrapped in the matrix.

The lattice strain has an opposite direction to lattice constant. Increasing the lattice strain leads to an increase in the internal forces/stresses which may oppose the crystal growth of magnetite. Thus, the crystallite size of magnetite, in case of FHP sample, will be slightly lowered than that in  $\text{FHPMn}_{0.5}$ ,  $\text{FHPMn}_{10}$ ,  $\text{FHPMn}_{20}$ ,  $\text{FHPMn}_{40}$  respectively; which is confirmed by TEM.

TEM of some selected samples are shown in Fig. 6. The crystallization of one or different phases is evidenced in TEM micrographs. TEM revealed precipitation of nano size rounded crystals of only magnetite phase dispersed in amorphous glassy phase in the quenched  $\text{FHPMn}_{0.5}$  and  $\text{FHPMn}_{20}$  samples. The crystallite size was increased by adding  $\text{MnO}_2$  as seen before from XRD analysis. Diffraction of  $\text{FHPMn}_{20}$  revealed crystallization of single phase, which mean the incorporation of Mn ions in magnetite.

### Magnetic properties

Fig. 7 and Table 2 illustrate the variation of hysteresis curves and magnetic values with heat treatment temperatures under a magnetic field of 25 kOe. It could be observed that all the samples exhibited a similar magnetic behavior, which is characteristic for soft magnetic materials, with a thin hysteresis cycle and low coercive field. Magnetite is the only crystallized phase regarded as ferromagnetic phase, accordingly, increasing or decreasing in  $M_s$  will be related to the amount of crystallized magnetite. FHP sample have the highest  $M_s$  value reaching 58.99 emu/g, this value was decreased to 38.59 emu/g by increasing the amount of  $\text{P}_2\text{O}_5$  added. These results reflect the effect of adding high quantity of  $\text{P}_2\text{O}_5$  on decreasing the degree of crystallinity in quenched samples. Addition of

40 gm Mn led to significant decrease in  $M_s$  to 23.94 emu/g, which can be attributed to incorporation of the lower magnetic element (Mn) in the higher magnetic one ( $\text{Fe}_3\text{O}_4$ ).

The remanence is the amount of magnetic materials which could be magnetized, even in the absence of external magnetic field. The remanence magnetization values were much lower than the saturation magnetization values. This could be due to structural features of glass-ceramic [16]. The coercive field

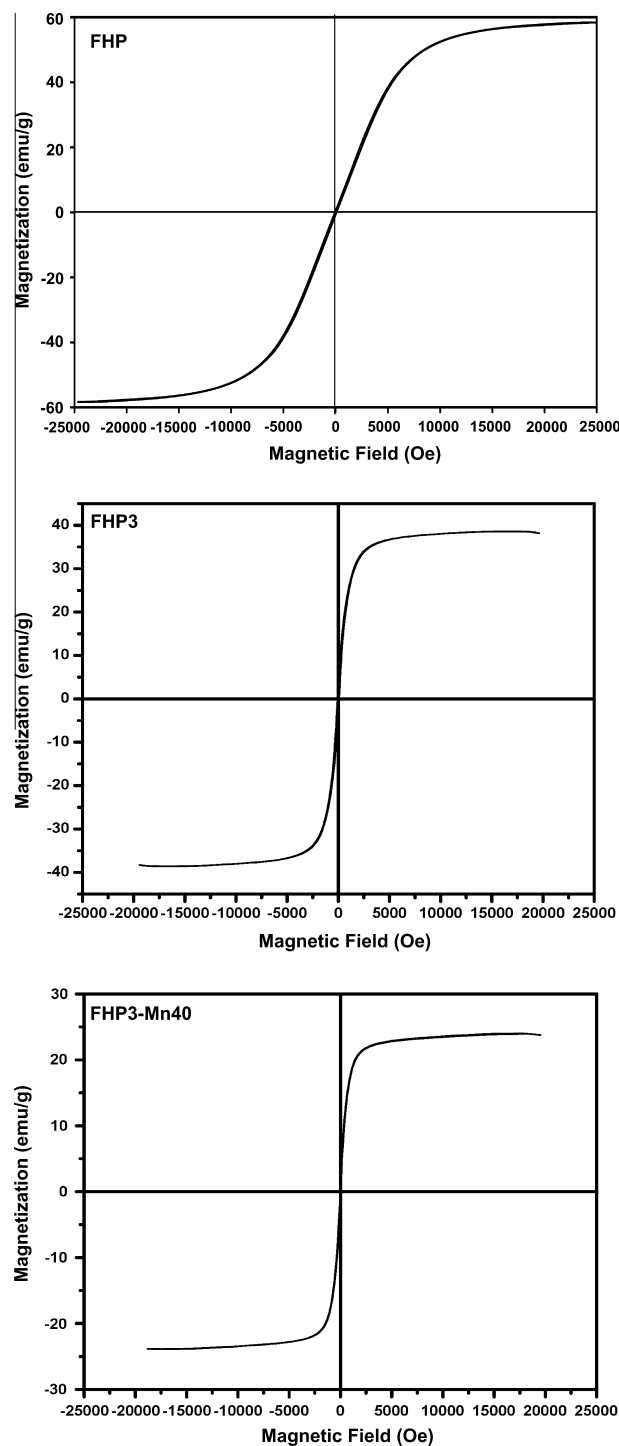


Fig. 7 Magnetic hysteresis of quenched samples under a maximum magnetic field of 25 kOe.

**Table 2** Magnetic properties of quenched samples under a maximum magnetic field of 25 kOe.

Sample no.	Magnetic properties		
	$M_s$ (emu/g)	$M_r$ (emu/g)	H <sub>c</sub> (Oe)
FHP	58.99	4.634	24.76
FHP3	38.59	3.32	76.494
FHPMn40	23.941	0.99	27.358

depends on the microstructure. In general, as the particle size increase the coercive field decrease.

#### Role of P<sub>2</sub>O<sub>5</sub>

It has been reported that, P<sub>2</sub>O<sub>5</sub> enhance the nucleation density and thus restricts the crystal growth and induces amorphous phase separation. P<sub>2</sub>O<sub>5</sub> can induce phase separation to promote heterogeneous nucleation and then produce a fine-grained interlocking morphology. The heterogeneous nucleation was favorable in reducing nucleation energy.

The addition of P<sub>2</sub>O<sub>5</sub>, greatly affects phase formation and morphology. It led to a slight increase in the peak crystallization temperature observed in DTA curves due to the reduction in the number of remaining sites available for magnetite crystallization, where most of the magnetite was crystallized from melt during cooling to room temperature.

Yinnon and Uhlmann [28] suggested that the nucleating agents could be selectively enriched in one separated phase thus providing the sites for nucleus. Ryerson and Hess [29] proposed that when a modifier cation is added in a silica melt, it is surrounded by both  $O_b$  and  $O_{nb}$ . This oxygen isolates the network-modifier cations from each other by providing screens that masks the positive charge. However, modifier cations that are partly or wholly coordinated by bridging oxygen are poorly shielded from each. Consequently, substantial coulombic repulsions occur between network-modifier cation with give rise to the enthalpy of unmixing and consequently lead to phase separation. Markhasev and Sedletskii [30] found that immiscibility fields expand with a decrease of the ionic radius of the modifier cation in binary silicate melt.

#### Role of MnO<sub>2</sub>

MnO<sub>2</sub> have a significant effect on lowering viscosity of the melt, so increasing amount of MnO<sub>2</sub> added leads to decreasing the melt viscosity and facilitating the mobility of different ions causing a relatively larger crystallite size as imprinted from XRD and TEM results. On the other hand, Mn ions can replace Fe ions and make it possible for higher amounts of magnetite to be crystallized.

#### Conclusions

A series of magnetic glass ceramics contains different additions of P<sub>2</sub>O<sub>5</sub> and/or MnO<sub>2</sub> in the system Fe<sub>2</sub>O<sub>3</sub>:ZnO:CaO:SiO<sub>2</sub>:B<sub>2</sub>O<sub>3</sub> were prepared. A significant decrease in the thermal effects was observed by adding P<sub>2</sub>O<sub>5</sub> and/or MnO<sub>2</sub>. XRD of quenched samples show crystallization of magnetite with particle size ~10–30 nm. Addition of MnO<sub>2</sub> enhanced crystallization of more magnetite during cooling from melting

temperature. Heat treatment at 800 °C for 2 h, under reducing atmosphere, caused an increase in the amount of the crystallized magnetite with the appearance of minor hematite and Ca<sub>2</sub>SiO<sub>4</sub>.  $M_s$  value reaching 58.99 emu/g. The prepared magnetic glass ceramics are expected to be useful for localized treatment of cancer.

#### Conflict of interest

*The authors have declared no conflict of interest.*

#### Compliance with Ethics Requirements

*This article does not contain any studies with human or animal subjects.*

#### Acknowledgment

This project was supported financially by the Science and Technology Development Fund (STDF), Egypt, Grant No. 240.

#### References

- [1] Bretcanu O, Verné E, Coisson M, Tiberto P, Allia P. Temperature effect on the magnetic properties of the co precipitation derived ferrimagnetic glass-ceramics. *J Magn Mater* 2006;300:412–7.
- [2] Ebisawa Y, Miyaji F, Kokubo T, Ohura K, Nakamura T. Bioactivity of ferrimagnetic glass-ceramics in the system FeO–Fe<sub>2</sub>O<sub>3</sub>–CaO–SiO<sub>2</sub>. *Biomaterials* 1997;18:1277–84.
- [3] Kokubo T, Hayashi T, Sakka S, Kitsugi T, Yamamuro T. Bonding between bioactive glasses, glass ceramics or ceramics in simulated body fluid. *Yogyo-Kyokai-Shi* 1987;95:785–91.
- [4] Cetas TC, Gross EJ, Contractor Y. A ferrite core/metallic sheath thermo seed for interstitial thermal therapies. *IEEE Trans Biomed Eng* 1998;45:68–77.
- [5] Jordan A, Scholz R, Wust P, Fähling H, Felix R. Magnetic fluid hyperthermia (MFH): cancer treatment with AC magnetic field induced excitation of biocompatible superparamagnetic nanoparticles. *J Magn Mater* 1999;201:413–9.
- [6] Gómez-Lopera SA, Plaza RC, Delgado AV. Synthesis and characterization of spherical magnetite/biodegradable polymer composite particles. *J Colloid Interf Sci* 2001;240:40–7.
- [7] Lee YK, Kim DH, Lee YJ, Kim KN, Shim IB. Ceramics, cells and tissues. In: Eighth annual seminar and meeting, Faenza; 2003.
- [8] Takegami K, Sano T, Wakabayashi H, Sonoda J, Yamazaki T, Morita S, Shibuya T, Uchida A. New ferromagnetic bone cement for local hyperthermia. *J Biomed Mater Res* 1998;43:210–4.
- [9] Borrelli et al. Radio frequency induced hyperthermia for tumor therapy, US Patent 4323056; 1982.

- [10] Kokubo T, Yamamuro T, Ebisawa Y, Ohura K. European patent 361797; 1990.
- [11] Oh SH, Choi SY, Lee YK, Kim KN. Research on annihilation of cancer cells by glass-ceramics for cancer treatment with external magnetic field. I. Preparation and cytotoxicity. *J Biomed Mater Res* 2001;54:360–5.
- [12] Ebisawa Y, Miyaji F, Kokubo T, Ohura K, Nakamura T. Surface reaction of bioactive and ferrimagnetic glass-ceramics in the system  $\text{FeO-Fe}_2\text{O}_3\text{-CaO-SiO}_2$ . *J Ceram Soc Jpn* 1997;105: 947–51.
- [13] Arcos D, del Real RP, Vallet-Regi M. A novel bioactive and magnetic biphasic material. *Biomaterials* 2002;23:2151–8.
- [14] O'Horo M, Steinitz R. Characterization of devitrification of an iron-containing glass by electrical and magnetic properties. *Mater Res Bull* 1968;3:117–25.
- [15] Auric P, Dang NV, Bandyopadhyay AK, Zarzycki J. Superparamagnetism and ferrimagnetism of the small particles of magnetite in a silicate matrix. *J Non-Cryst Solids* 1982;50: 97–106.
- [16] Bretcanu O, Spriano S, Verné E, Coisson M, Tiberto P, Allia P. The influence of crystallized  $\text{Fe}_3\text{O}_4$  on the magnetic properties of co precipitation-derived ferrimagnetic glass-ceramics. *Acta Biomater* 2005;1:421–9.
- [17] Ebisawa Y, Sugimoto Y, Hayashi T, Kokubo T, Ohura K, Yamamuro T. Crystallization of  $(\text{FeO}, \text{Fe}_2\text{O}_3)\text{-CaO-SiO}_2$  glasses and magnetic properties of their crystallized products. *Seram Ronbun* 1991;1:7–13.
- [18] Kuwashita M, Iwahashi Y, Kokubo T, Yao T, Hamada S, Shinjo T. Preparation of glass-ceramics containing ferrimagnetic zinc-iron ferrite for the hyperthermal treatment of cancer. *J Ceram Soc Jpn* 2004;112:373–9.
- [19] Wu C, Chang J, Zhai W. A novel hardystonite bioceramic: preparation and characteristics. *Ceram Int* 2005;31:27–31.
- [20] Hessian MM, Rashad MM, ElBarawy K, Ibrahim IA. Influence of manganese substitution and annealing temperature on the formation, microstructure and magnetic properties of Mn-Zn ferrites. *J Magn Magn Mater* 2008;320:1615–21.
- [21] Papazoglou P, Eleftheriou F, Zaspalis VT. Low sintering temperature MnZn-ferrites for power applications in the frequency region of 400 kHz. *J Magn Magn Mater* 2006;296:25–31.
- [22] Abdel-Hameed SAM, Hessian MM, Azooz MA. Preparation and characterization of some ferromagnetic glass-ceramics contains high quantity of magnetite. *Ceram Int* 2009;35: 1539–44.
- [23] Arvind A, Sarkar A, Shrikhande VK, Tyagi AK, Kothiyal GP. The effect of  $\text{TiO}_2$  addition on the crystallization and phase formation in lithium aluminum silicate (LAS) glasses nucleated by  $\text{P}_2\text{O}_5$ . *J Phys Chem Solids* 2008;69(11):2622–7.
- [24] Karamanov A, Pelino M. Crystallization phenomena in iron-rich glasses. *J Non-Cryst Solids* 2001;281:139–51.
- [25] Klug HP, Alexander LE. X-ray diffraction procedures for polycrystalline and amorphous materials. New York: Wiley; 1974.
- [26] McMillan PW. Glass ceramics. 2nd ed. London: Academic Press; 1979.
- [27] Hammond C. The basic of crystallography and diffraction. New York: Oxford University Press; 1997.
- [28] Yinnon H, Uhlmann DR. A kinetic treatment of glass formation V: surface and bulk heterogeneous nucleation. *J Non-Cryst Solids* 1981;44:37–55.
- [29] Ryerson FJ, Hess PC. The role of  $\text{P}_2\text{O}_5$  in silicate melts. *Geochim Cosmochim Acta* 1980;44:611–24.
- [30] Markhasev BI, Sedletskii ID. Dokl Akad Nauk SSSR (Engl Transl) Chem Sect 1963;148:112.